Open access • Journal Article • DOI:10.1029/95JC02901

Circulation near submarine canyons: A modeling study — Source link

John M. Klinck

Published on: 15 Jan 1996 - Journal of Geophysical Research (John Wiley & Sons, Ltd)

Topics: Submarine canyon, Canyon, Stratification (water), Stratified flow and Downwelling

1-1996

Circulation Near Submarine Canyons: A Modeling Study

John M. Klinck
Old Dominion University, jklinck@odu.edu

Original Publication Citation

Klinck, J.M. (1996). Circulation near submarine canyons: A modeling study. *Journal of Geophysical Research-Oceans, 101*(C1), 1211-1223. doi: 10.1029/95jc02901

JOURNAL OF GEOPHYSICAL RESEARCH, VOL. 101, NO. C1, PAGES 1211–1223, JANUARY 15, 1996

Circulation near submarine canyons: A modeling study

John M. Klinck
Department of Oceanography, Center for Coastal Physical Oceanography, Old Dominion University, Norfolk, Virginia

Abstract. Circulation near a submarine canyon is analyzed with a numerical model. Previous theoretical work indicated that stratification controlled the interaction of coastal flow with canyons, specifically, the ratio of canyon width to the internal radius of deformation. A wide canyon was thought to merely steer the flow, while a narrow canyon would create substantial cross-shelf exchange. Four cases are analyzed considering two directions of alongshore flow and two choices of initial stratification. The weakly stratified case has an internal radius about equal to the canyon width, while the strongly stratified case has one about 3 times the canyon width. The direction of the alongshore flow is shown in this study to be the more important of the two factors. In particular, right-bounded flow (flow with the coast on the right, looking downstream in the northern hemisphere) leads to shallow downwelling in the canyon and weak exchange across the shelf break, while left-bounded flow creates upwelling at the head of the canyon and strong exchange between the ocean and shelf. In left-bounded flow (upwelling), dense water is pumped onto the shelf, even for strong stratification. However, the stratification limits the vertical extent of the topographic influence so that the alongshore flow above the canyon is only weakly affected in the strongly stratified case. With any level of stratification the surface temperature (density) is not modified at all by the flow interaction with the submarine canyon. The important dynamics involve pressure gradients and Coriolis acceleration and how they interact with the bathymetric gradients but not advection of momentum. Advection of density is clearly important in the upwelling cases. Finally, continued upwelling onto the shelf acts as a drag mechanism and retards the alongshore coastal flow.

1. Introduction

In the past, water circulation in submarine canyons was ignored, largely because of the size of these features and because larger-scale circulation on the continental shelves was poorly understood. What studies of canyon circulation existed focused on sediment transport driven by tidal oscillations, so observations tended to be taken a few meters from the bottom for a few tidal cycles [*Inman et al.*, 1976]. In more recent times some direct observations of water motion in and around canyons have been made; but because of the complexity of the observed flow patterns, there has been a tendency to avoid submarine canyons when studying shelf circulation. The result is that the dynamical processes responsible for the flow near submarine canyons is rather poorly understood [*Hickey*, 1995].

The first indication of the influence of submarine canyons on coastal circulation was the observation of a persistent pool of dense water on the shelf near Vancouver Island [*Freeland and Denman*, 1982]. Analysis of the properties of this water showed that it had come from offshore and from depths of more than 400 m. At the time of the observed upwelling the flow along the outer shelf was southward. A model was proposed that the flow up the canyon was driven by the geostrophic pressure gradient of the coastal circulation. A second study in this area [*Freeland and McIntosh*, 1989] found that the alongshore flow at the edge of the shelf creates a pressure gradient that forces water up the submarine canyon. Along the onshore section of the canyon, bottom slope drives water upward, creating vortex stretching and cyclonic circulation.

A study of circulation and sediment transfer in Quinault Canyon off the U.S. northwest coast [*Hickey et al.*, 1986] found that subtidal variations in the circulation in the canyon and vertical excursion of turbidity within the canyon were correlated with variations in the alongshore flow. A similar study in Astoria Canyon (B. Hickey, Response of a narrow submarine canyon to strong wind forcing, submitted to *Journal of Physical Oceanography*, 1995] (hereinafter referred to as submitted manuscript, 1995), also located on the U.S. north-

Paper number 95JC02901.
0148-0227/96/95JC-02901$05.00

west coast, analyzed the response to wind-driven reversal of the alongshore flow. Left-bounded flow was shown to create strong upwelling and cyclonic circulation within the canyon. Weak alongshore flow seemed to result in a closed circulation above the canyon. For stronger flow there was only a weak disturbance over the canyon.

Baltimore canyon is typical of submarine canyons on the U.S. northeastern coast which are 10 km in width and about 3 times as long as they are wide. *Hunkins* [1988] demonstrated several peculiarities of canyon circulation. The mean alongshore flow above the level of the surrounding shelf is unaffected by the presence of the canyon. Within the canyon the time mean current can be upcanyon or downcanyon. Water motion in the upper canyon is along the canyon axis and toward the head of the canyon (upwelling), while that at the mouth of the canyon is along isobaths creating an anticyclonic circulation. In Lydonia Canyon, another example of a U.S. northeastern coast canyon [*Noble and Butman*, 1989], flow above the shelf depth is unaffected by the canyon bathymetry. However, empirical orthogonal function (EOF) modes of across-shore flow (on the shelf and in the canyon) are correlated with the alongshore flow, consistent with the idea that current along the axis of the canyon is forced by the geostrophic pressure gradient of the overlying flow.

Grand-Rhône Canyon on the Mediterranean coast of France [*Durrieu de Madron*, 1994] is characterized by different oceanographic conditions, with the strong alongshore current being along the shelf slope and not up on the shelf. However, general results show that the flow across the mouth of the canyon (the canyon is on the right, looking downstream) creates a pressure gradient that forces water out of the canyon. Such downaxis flows were identified by turbidity and water mass characteristics as well as with direct current measurements. One interesting observation is that while the alongshore flow turns into the outer part of the canyon, there is an anticyclone within the inner canyon which could be driven by the downwelling or by frictional coupling with the alongshore flow. Multiple circulation cells within submarine canyons had not been reported previously.

These observational studies are summarized as follows. The large-scale flow in coastal areas is generally alongshore, parallel to isobaths. If the isobaths curve sharply, where the internal radius of deformation provides the scale for comparison [*Klinck*, 1988, 1989], then flow within the canyon is driven, generally along the axis of the canyon, by the geostrophic pressure gradient of the overlying alongshore flow. For a narrow canyon the flow in the canyon is parallel to the central axis and the bottom slope creates vertical water motion. Left-bounded alongshore flow (coast to the left, looking downstream) creates upwelling while right-bounded flow creates downwelling. For weakly curving isobaths or even wide canyons, current follows isobaths without generating strong vertical circulation. However, the circulation above the canyon seems to cross the canyon, with no interaction.

These ideas are considered in the remainder of this paper with a numerical model of flow near a submarine canyon. The purpose is to analyze the effect of changes in stratification and direction of alongshore flow on the circulation in and near submarine canyons. In particular, two choices of initial stratification create radii of deformation that are comparable to and 3 times the canyon width. For each of these choices, two directions of alongshore flow are imposed. The remainder of the paper is organized in sections, with the next section describing the numerical model and the parameter choices made for this study. Section 3 presents the simulated circulation for the four cases. The area-integrated transport along certain control planes as a function of time is also presented. Section 4 considers the implications of the model simulations and comments on the proposed dynamics of interaction of alongshore flow with submarine canyons. The final section presents the conclusions.

2. Description of Numerical Model

Simulations presented in this paper were made with version 3.0 of the semispectral primitive equation model (SPEM) described by *Haidvogel et al.*, [1991]. This model is designed for circulation in an environment with strong changes in bottom topography, weak friction and nonlinear dynamics. A detailed description of the model is given by *Haidvogel et al.*, [1991].

The simulations were conducted in a domain (Figure 1) that is 96 km in the alongshore direction x and 64 km in the across-shore direction y. The domain is periodic in the alongshore direction to avoid problems with open boundary conditions. However, for sufficiently long simulations the possibility exists for the disturbance created by the canyon to pass through the periodic bound-

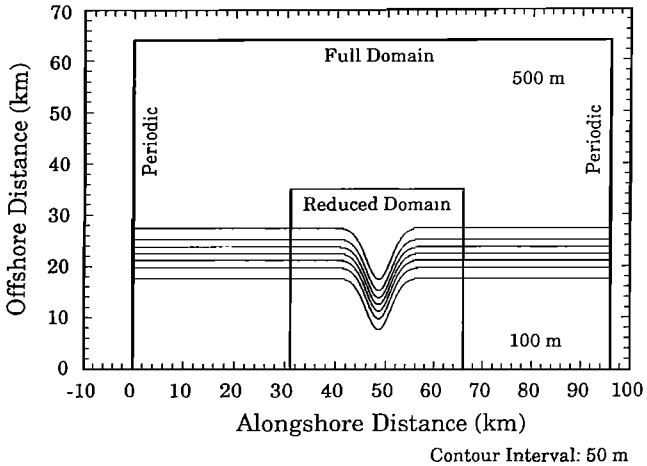

Figure 1. Model domain and bottom topography. The larger box is the full domain; the smaller box surrounding the canyon is the reduced area for figures. The coastal area near the bottom of the figure is 100 m deep, and the offshore ocean near the top is 500 m deep. The contour interval for the isobaths is 50 m.

ary and appear upstream. The domain was chosen to be large enough that such upstream disturbances are delayed (details below). Because of the small scale of submarine canyons, the model grid spacing was chosen to be 0.5 km uniformly in both directions. The vertical structure of the circulation is represented by 7 spectral functions, which is comparable to 13 levels in the vertical. Some test cases with this model geometry using larger numbers of functions showed no real differences in the resulting flow.

The bottom topography represents a continental shelf with a uniform shape in the alongshore direction that is cut by a single canyon. The shelf is nominally 100 m deep, and the offshore ocean is 500 m deep. At any alongshore x location the depth is defined as

$$H(x,y) = H_m - \frac{H_s}{2}\left[1 - \tanh\frac{y - y_o(x)}{a}\right], \quad (1)$$

where $H_m(= 500$ m) is the maximum depth, $H_s(=$ 400 m) is the depth change from the shelf to the ocean, $y_o(x)$ is the location of the shelf break (defined below), and $a(= 5$ km) is a transition scale defining the shelf slope. The location of the shelf break is

$$y_o(x) = y_n + y_b\left[1 - e^{\frac{-(x^2 - x_o^2)}{2b^2}}\right], \quad (2)$$

where $y_n(= 12$ km) is the nominal distance of the head of the canyon from the coastal wall, $y_b(= 10$ km) is the distance added to y_n to reach the shelf break, $x_o(=$ 48 km) is the location of the centerline of the canyon, and $b(= 2.5$ km) is a width scale for the canyon. These choices produce a canyon that is approximately 10 km wide at the mouth and 20 km from the mouth to the head (Figure 1).

Dependent variables are the three components of flow along with temperature; salinity does not vary in the simulations. A linear equation of state is specified, so density is proportional to temperature. The circulation occurs in a uniformly rotating environment ($f = 10^{-4}$ s^{-1}); the domain is too small and the duration of the simulations is too short for the latitudinal variation of the Coriolis parameter f to play any role.

Although vertical viscosity is thought to be important in shallow water, it was ignored in these simulations in order to reduce the number of processes being considered and to avoid having to choose poorly known parameters (the turbulent viscosities). The implication of this choice is that there is no bottom Ekman layer which might provide additional flow across isobaths.

The interaction of the circulation with the bathymetry produces considerable gravity wave energy, so weak horizontal diffusion of momentum (proportional to the Laplacian of the flow) is introduced with a diffusivity of 20 m^2 s^{-1} to absorb this high-frequency motion. Since temperature (density) advection is critical to the circulation, a more scale selective dissipation is imposed on temperature in the form of biharmonic diffusion with a coefficient of 5.0×10^5 m^4 s^{-1}.

The initial state of the model is rest with a linear vertical density stratification. The initial temperature is

$$T(z, t = 0) = 20.0 + \Delta T\frac{z}{500}, \quad (3)$$

where z is the depth in meters (note that z is positive upward) and ΔT is the top-to-bottom temperature difference. Temperature difference converts to density difference by the equation of state ($\Delta\rho = -0.14\,\Delta T$). It is convenient to classify the stratification by the internal radius of deformation ($\lambda = N\,H/f$), where N is the buoyancy frequency, H is the depth, and f is the Coriolis parameter. The square of the buoyancy frequency is calculated as $N^2 = -g\,\Delta\rho/\rho_o\,H$. The two choices for the initial temperature difference (1°C and 16°C) give rise to internal radii of 8.1 and 32.7 km, respectively. These choices were made so that the radii would be comparable to and 3 times the canyon width. These stratification values generally cover the observed range of coastal stratification, where the smaller difference produces a stratification that is weaker than observed, while the larger creates the strongest observed stratification.

SPEM has a rigid lid which requires the determination of the barotropic stream function, which is proportional to the surface pressure, by the solution of an elliptic differential equation at every model time step. The stream function value on the offshore wall (the stream function is zero on the coastal wall) controls the cross-shore pressure difference and thereby the net alongshore transport. However, the structure of the alongshore flow is determined by the model dynamics and the bottom topography. For these simulations the offshore stream function was chosen to ramp up over a period of about 10 days,

$$\psi(y = 64\text{ km}) = \psi_o\frac{1}{2}\left[1 + \tanh\frac{t - 6}{3}\right], \quad (4)$$

where $\psi_o = \pm 2.5 \times 10^6 m^3\ s^{-1}$ is the asymptotic value and the time t is expressed in days. This mechanism creates a uniform alongshore flow of about 0.1 m s^{-1} after about 10 days.

Four simulations are analyzed for the two choices of initial stratification and direction of the alongshore flow, with the cases designated as weakly or strongly stratified and upwelling or downwelling, depending on the direction of alongshore flow. Three of the cases were integrated with a time step of 270 s for 40 model days, saving the model state every 5 days. However, the strongly stratified, upwelling case required a time step of 100 s (because of the faster internal waves) for the first 5 days and 50 s for an additional 10 days. This simulation was difficult because the upwelling created a dense water plume on the shelf along the coastal wall. A temperature front at the nose of the plume sharpened until by day 15 the front was too sharp to be resolved by the model grid. By this time the plume was three quarters of the way around the model domain and was beginning to interact with the canyon. It would have been possible to increase horizontal diffusion to coun-

teract the sharpening of the front, but the purpose of the simulation was served by the 15 days of simulation.

Because these simulations use a periodic domain, it is important to determine the time required for disturbances to travel around the model domain (96 km). There is no surface gravity wave to be concerned about in SPEM because of the rigid lid. The internal wave speed can be estimated as $c_i = \sqrt{g' H}$, where H is the depth (ranging from 100 m on the shelf to 500 m in the ocean) and $g' = g \Delta\rho/\rho_o$ is the reduced gravity. Thus the internal wave speed for weakly stratified cases ranges from 0.36 to 0.82 m s^{-1}, while the strongly stratified cases have a range of 1.46 to 3.27 m s^{-1}. The weakly stratified internal waves can circle the model in 1.35 to 3.1 days, while the strongly stratified waves take 0.36 to 0.82 days. It is clear that the internal gravity waves circle the domain many times during the 10 days of spin-up, but recall that these waves are created by initial transients and are preferentially damped.

A second wave to consider is the trapped topographic vorticity wave which can have a number of wave structures, depending on the bottom shape and the stratification. The characteristics of these waves are determined with software developed by *Wilkin* [1987] and used by *Wilkin and Chapman* [1990]. Owing to the small domain, the fastest waves in the model domain in any mode are the longest allowed which have a wavelength of 96 km. The fastest modes have speeds of 1.24 and 0.79 m s^{-1} for the strongly and weakly stratified cases, respectively. These waves travel around the domain in about 1.0 and 1.5 days, respectively. The slower waves (higher modes and shorter waves) have speeds as slow as 0.1 m s^{-1}, which is comparable to the speed of the net flow. These waves clearly circle the domain several times during the simulations, thus contaminating the solution. The downwelling cases do not show any accumulation of vorticity that might be due to these waves. The upwelling cases, however, allow the possibility that some of the shelf waves may be caused to stand by the opposing mean flow, and there is some indication in the results that localized standing disturbances occur. However, no obvious effects occur that mask the direct interaction of the flow with the canyon bathymetry.

A final speed to be concerned about is advection. Forcing creates an alongshore flow of 0.1 m s^{-1} which carries water around the domain in 11.1 days. The strongest current in the simulations is along the coastal wall at about 0.2 m s^{-1}, giving an advection time of about 5 days. The potential exists for the flow in the vicinity of the canyon to be influenced by the wraparound flow after 15 days or so. This turns out not to be a problem, except for the strongly stratified, upwelling case, as we will see from the model results.

3. Results

Four situations are considered to illustrate the effect of submarine canyons on alongshore flow which involve choices of initial stratification and flow direction. The model exhibits the following two general phases of adjustment: spin-up and adjustment. This behavior is best illustrated by the transport calculations that are described below. Spin-up occurs over the first 10 days of the simulation for all cases, and this is controlled by the time development of the offshore stream function value. Beyond day 10 the simulations adjust to the alongshore flow and the nature of the adjustment is rather different for the two directions of alongshore flow. The downwelling cases undergo a slow frictional decay in speed, while the upwelling cases adjust more rapidly owing to the dense water being deposited on the shelf (discussed in detail below).

The general character of the circulation is established by model day 10 for all cases, and this is the best time to describe the effect of the canyon on the imposed flow. It is not really appropriate to look for the long-term steady state, as the circulation on the shelf rarely remains constant for extended periods. Additionally, the wraparound flow can become important after this time, further clouding the dynamics.

Each of these cases is described by the horizontal velocity at two levels, middepth on the shelf (52.5 m) and below the shelf break (127.5 m). The vertical velocity just below the shelf depth (105 m) is useful to indicate exchange between the canyon and the adjacent shelf. Finally, the cumulative effect of vertical motion is shown by the temperature structure above the shelf (95 m). The "odd" depths are chosen to match (or split) various horizontal planes (at depths of 105 and 150 m) through which transport is calculated. The flow is displayed at the midpoint of these levels, and the vertical velocity is shown at the top of the canyon.

3.1. Weakly Stratified, Downwelling Case

This case has an initial temperature difference of 1°C over 500 m and alongshore flow is driven to the right, looking offshore (right-bounded). After 10 days of forcing the circulation at middepths over the shelf (52.5 m) is everywhere toward the right (looking offshore) about 0.1 m s^{-1}, except over the canyon where the flow exhibits a cyclonic turn (Figure 2a). The circulation is weak over the center of the canyon and is larger at the head of the canyon (up to 0.2 m s^{-1}). Currents below the shelf break (127.5 m) have largely the same characteristics (Figure 2b) as those above. Around the rim of the canyon the current is about double the speed of that offshore; the horizontal circulation over the center of the canyon is weak. The vertical velocity just below the shelf is rather antisymmetrical (Figure 2c), with downwelling on the upstream (left) side of the canyon and upwelling on the downstream side. There is a small upwelling near the upstream corner of the canyon and a corresponding downwelling area downstream of the canyon. The largest downward speed (-0.0016 m s^{-1}) is larger than the largest upward speed (0.0011 m s^{-1}), so even though the spatial pattern is antisymmetric, there is a net downward displacement for particles.

The temperature change relative to the initial temperature at this depth (95 m) is everywhere warmer

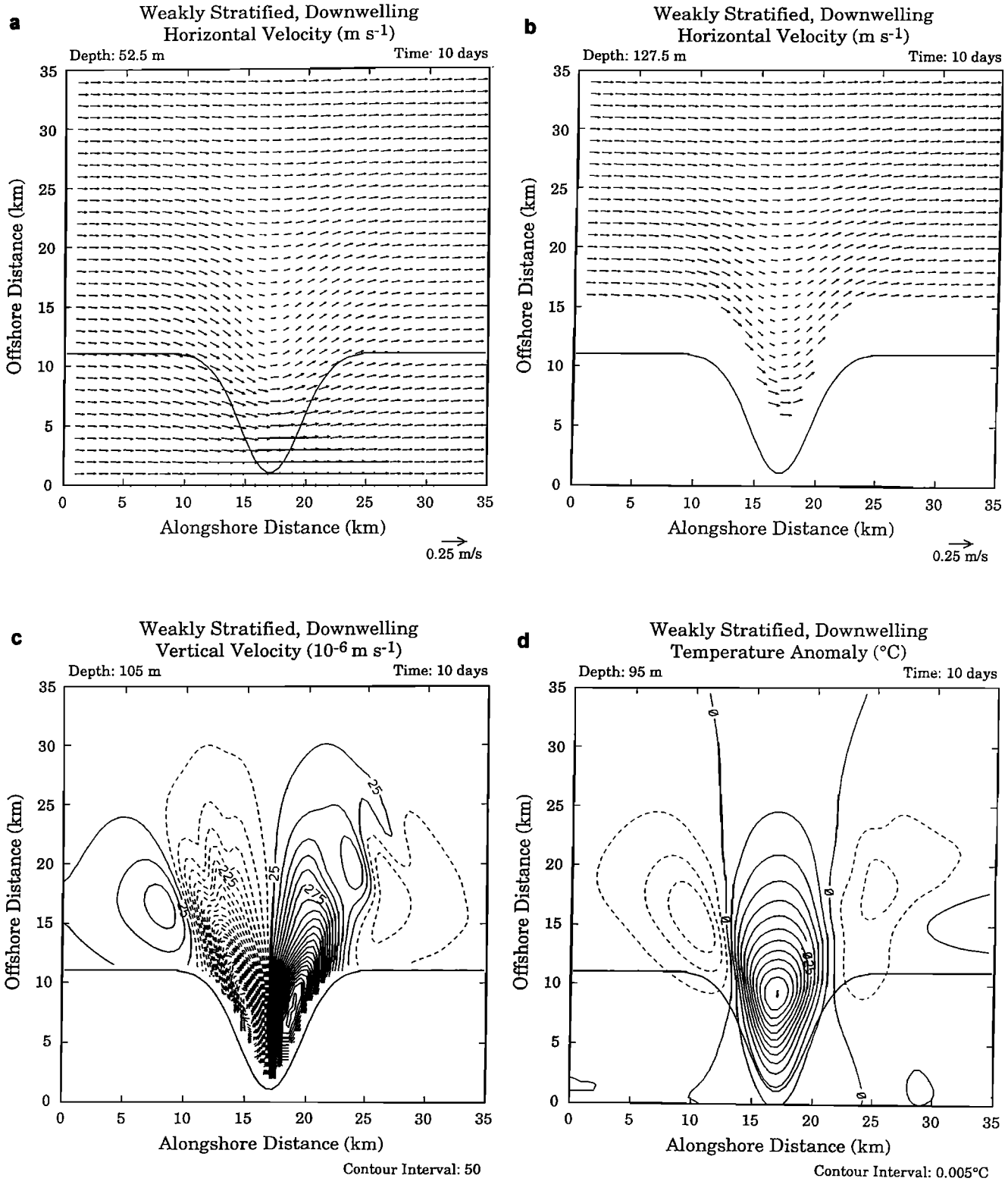

Figure 2. Model solution for the weakly stratified, downwelling case at day 10. The solid line is the 105-m isobath, indicating the shelf break and the top of the canyon. (a) The horizontal velocity vectors over the shelf at a depth of 52.5 m. (b) The horizontal velocity vectors below the shelf at a depth of 127.5 m. (c) The vertical velocity (multiplied by 10^6) just below the shelf (105 m). The solid lines indicate positive (upward) flow, and the dashed lines show negative flow. (d) The temperature anomaly above the shelf at 95 m. The anomaly is the temperature change from its initial value at this depth (= 19.81°C).

than the water at the same depth offshore (Figure 2d), consistent with a general downwelling within the canyon. It is evident that the modifications of the temperature are confined to the vicinity of the canyon. On either side of the canyon there are regions of cooler, upwelled water (about 0.02°C cooler than at the beginning of the simulation).

The general structure of this circulation pattern is that the alongshore flow follows isobaths, even in the canyon, where the water accelerates around the rim of the canyon, slipping deeper on the upstream rim, and returning upward on the downstream rim. The largest vertical distance for a fluid particle (estimated from the temperature change (about 0.075°C) divided by the initial temperature gradient (1°C over 500 m)) is about 37.5 m. For this case the effect of the canyon is localized.

3.2. Strongly Stratified, Downwelling Case

The strongly stratified, downwelling simulation is a repeat of the previous case, except that the initial vertical temperature difference is 16°C. The horizontal flow above the shelf (52.5 m) is very uniform with a speed of about 0.1 m s^{-1} (figure not shown). There is a slightly perceptible disturbance over the canyon having a slight amount of cyclonic turning. The deeper flow (127.5 m) is also very uniform away from the canyon (figure not shown) with a speed of about 0.1 m s^{-1}. Within the canyon the circulation is rather weak, except for an increase in speed around the edge of the canyon. The vertical speed below the shelf break (105 m) is antisymmetrical with downwelling on the upstream side of the canyon and upwelling on the downstream side (Figure 3). The strongest vertical speed is along the rim of the canyon, and the maximum downwelling is stronger than the maximum upwelling (-0.00086 versus 0.00051 m s^{-1}). There is more small-scale structure in the vertical velocity that is due to internal waves which are supported by the stronger stratification. The major distortion of the temperature (density) is within the canyon (figure not shown), where there is a strong downward displacement of the isotherms. The largest temperature anomaly occurs at the head of the canyon and decreases monotonically toward the open ocean. Weak upwelling occurs at the shelf break both up- and downstream of the canyon.

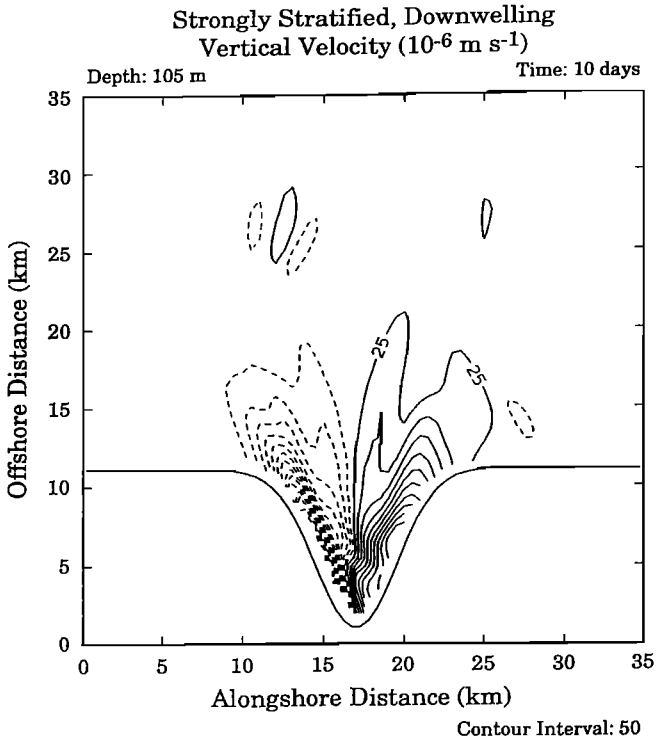

Figure 3. The vertical velocity just below the shelf break (105 m) for the strongly stratified, downwelling case at day 10. The solid line is the 105-m isobath, indicating the shelf break. The solid lines indicate positive (upward) flow, and the dashed lines show negative flow.

Although there is more structure in the circulation in this case, the general flow pattern is similar to the previous case, with some of the alongshore flow turning into the canyon and descending until it reaches the axis of the canyon. The flow then ascends through the downstream side of the canyon to rejoin the alongshore flow. The largest vertical excursion of isotherms is 23.1 m at the head of the canyon (estimated from a temperature change of 0.74°C).

3.3. Weakly Stratified, Upwelling Case

The weakly stratified, upwelling case has an initial temperature difference of 1°C. The reversal of the direction of the alongshore flow has a major effect on the character of the resulting circulation. Far offshore (more than 30 km from the coast) and upstream of the canyon, the flow above the shelf (52.5 m) is generally uniform with a speed of 0.1 m s^{-1} (Figure 4a). Over the canyon, however, the flow is everywhere onshore, leading to the formation of a strong jet along the coastal wall (speeds above 0.2 m s^{-1}). Downstream of the canyon, there is a region of very weak current between the middle shelf and the shelf break. Offshore of the shelf break, the flow executes an anticyclonic turn offshore. Notice also that the current along the shelf upstream of the canyon is weaker than that offshore of the shelf break. The circulation below the shelf (127.5 m) reinforces the idea of water turning toward the coast within the canyon (Figure 4b). Much of this water moves onto the shelf, while the rest turns offshore to continue alongshore. There is a weak cyclone downstream of the canyon. In spite of the strong distortion of the flow near the canyon, the alongshore flow is generally undisturbed more than 20 km (about 2 internal radii) offshore of the shelf break.

Water movement is upward everywhere at the top of the canyon (Figure 4c), except along the upstream rim, where there is a narrow band of downwelling. The region of general upwelling extends well offshore along the canyon centerline. At the downstream corner of the canyon along the shelf and offshore, there is a region of downwelling. The largest upward motion in the canyon occurs along the downstream rim with a

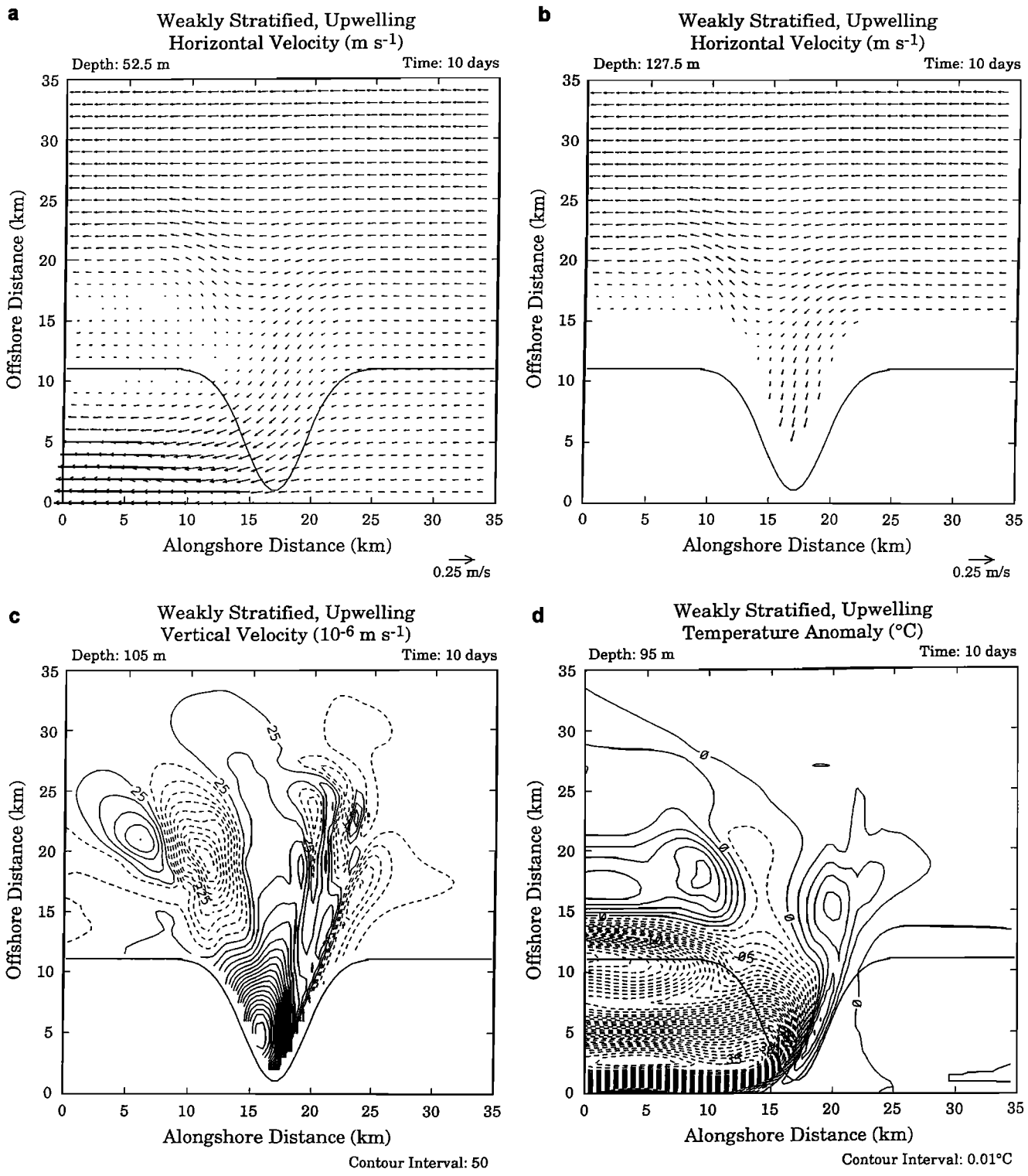

Figure 4. Same as Figure 2, except for the weakly stratified, upwelling case.

strength of 0.001 m s^{-1}. The upwelling within the canyon is clearly indicated by the low temperature over the canyon and downsteam (Figure 4d). The plume of cold water (0.4°C colder than the initial temperature) clearly comes from the head of the canyon and floods the shelf. A second region of cold water occurs along the shelf break downstream of the canyon. The downwelling on the downstream side of the canyon along the shelf break is evident as a warmer temperature.

The general character of the circulation in this upwelling case involves undisturbed upstream flow that turns into the canyon and splits into two parts. One part continues into the canyon, moving upward all the while, exiting at the head of the canyon to become a jet

along the coastal wall. A second, smaller branch turns toward the canyon, deflects offshore and then continues parallel to the coast. A small cyclone is trapped at the shelf break just downstream of the canyon. The largest vertical excursion of a water particle is estimated to be 192.5 m from a temperature change of 0.385°C.

3.4. Strongly Stratified, Upwelling Case

This final case reconsiders the previous case, with a strongly stratified fluid having an initial temperature difference of 16°C. The circulation at middepth (52.5 m) over the shelf is rather uniform at about 0.1 m s^{-1} (figure not shown). There is a slight cyclonic turn over the canyon and a perceptible increase in speed along the coastal wall downstream of the canyon, but otherwise, there is almost no indication of a disturbance. The circulation below the shelf (127.5 m) is very uniform offshore, with a strong turning of the flow into the canyon on the upstream side (figure not shown). As in the previous case, the water that enters the canyons splits into two parts, one that continues the cyclonic turn toward the head of the canyon and another part that turns anticyclonically and exits the canyon. Strong upwelling occurs over the whole top of the canyon (Figure 5). Two small centers of downwelling are evident at the upstream corner and just downstream of the canyon; however, the vertical speed in these areas is small. The largest upward speed in the canyon is 0.004 m s^{-1}, with the largest downward speed about half that value. Near the top of the canyon (95 m) the coldest water occurs along the upstream rim near the head of the canyon (figure not shown). There are two pools of warmer water just up- and downstream of the canyon, corresponding to the downwelling centers.

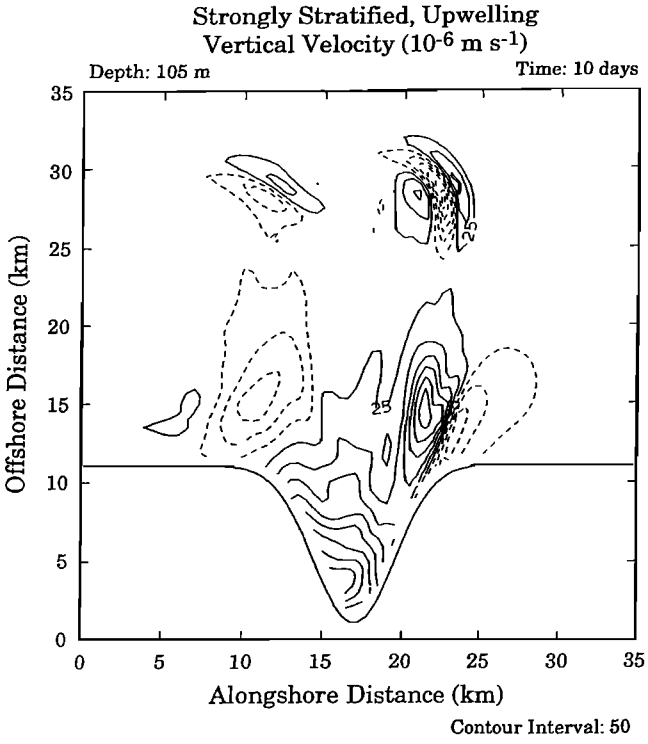

Figure 5. Same as Figure 3, except for the strongly stratified, upwelling case.

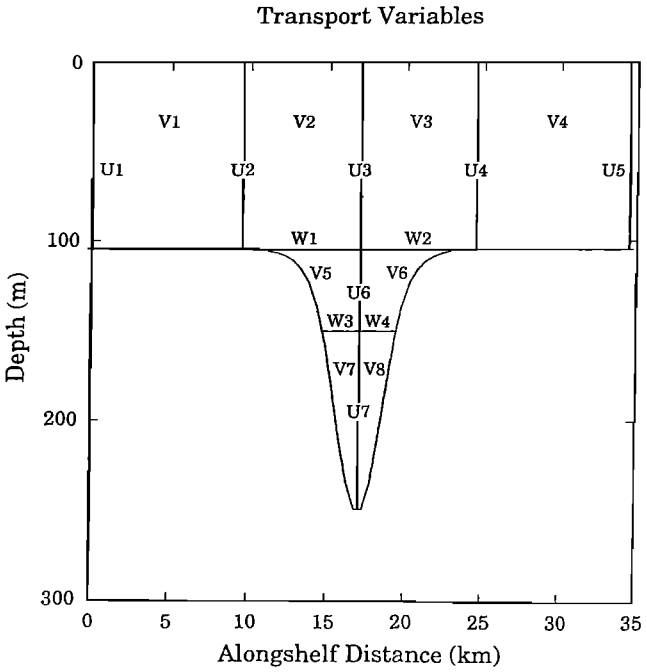

Figure 6. Planes for the volume transport calculation. The plane is located at the shelf break (depth of 105 m) which is 11 km offshore of the coastal wall. The alongshore transports U are calculated along seven vertical planes stretching from the shelf break to the coastal wall. The cross-shore transports V are calculated over eight vertical planes. The vertical transports W are calculated across four horizontal planes which stretch from the shelf break to the coastal wall.

The general circulation for this case has water turning into the canyon and much of it upwelling onto the shelf. The offshore distance over which the density field is disturbed by the canyon is larger than the previous case, reflecting the larger internal radius of deformation. The lowest temperature at the head of the canyon is about 1.14°C colder than the initial temperature, implying a vertical excursion of about 35.6 m.

3.5. Transport Calculation

The four simulations described above result in different volumes of water being exchanged vertically and horizontally. Volume transport is calculated along a series of planes (Figure 6), chosen to estimate exchange between the ocean and the shelf. A natural plane to chose is one aligned with the shelf break; the specific location is along the isobath on the undisturbed shelf associated with the depth 105 m, which is 11 km offshore of the coastal wall. Five cross-shelf planes divide the shelf into four regions. These planes are located at either end of the reduced model domain to characterize the alongshelf transport away from the canyon, just up- and downstream of the canyon and along the central axis of the canyon. Vertical transport is estimated over two horizontal planes, one covering the canyon just

Table 1. Transport Across All Planes at Day 10 for the Four Model Cases Plus the Strongly Stratified, Upwelling Case Without Momentum Advection.

	W/D	S/D	W/U	S/U	S/U/L
U_1	102.22	105.49	-125.38	-103.65	-79.18
U_2	116.52	113.08	-122.31	-104.38	-89.79
U_3	128.43	116.36	-86.62	-88.26	-111.64
U_4	117.93	112.79	-60.18	-73.49	-89.52
U_5	105.52	106.03	-57.50	-72.64	-83.11
U_6	23.91	13.68	-7.65	-2.19	-5.02
U_7	10.35	2.16	1.11	0.46	-0.94
V_1	-14.30	-7.59	-3.07	0.73	10.61
V_2	-33.72	-12.42	-16.90	-8.71	27.07
V_3	30.70	11.69	-22.12	-10.79	-20.05
V_4	12.42	6.76	-2.68	-0.85	-6.41
V_5	-7.28	-4.36	-6.55	-4.68	-0.21
V_6	7.75	5.25	-7.37	-5.54	-6.45
V_7	-5.18	-2.34	-5.70	-1.00	0.95
V_8	6.31	2.47	-3.49	-0.16	-1.58
W_1	-21.81	-9.14	18.80	7.41	5.22
W_2	20.21	8.12	4.32	3.98	2.07
W_3	-5.17	0.17	4.57	0.54	-0.01
W_4	4.04	-0.31	4.60	0.63	0.64

Units are 10^3 m^3 s^{-1}. Headings indicate weak (W) or strong (S) stratification, upwelling (U) or downwelling (D) and linear (L) dynamics. U, V, W are alongshore, cross-shore and vertical transports, respectively. Subscript numbers denote the plane (Figure 6) for which the transport is calculated.

below the shelf (105 m) and a second at 150 m (a somewhat arbitrary choice, but it divides the canyon into four volumes of about the same size).

The total transport is calculated normal to each of these planes (see Figure 6 for the symbols used for each transport calculation) by numerically integrating the model solution at 5-day intervals. The transport calculations are described below, and values for all of the simulations on day 10 are given in Table 1. The time histories of vertical transport for two cases are displayed in Figures 7 and 8.

3.5.1. Weakly stratified, downwelling. Transport across every plane for the weakly stratified, downwelling case increases rapidly to day 15 and decline weakly thereafter (Figure 7). The alongshore transport at day 10 (Table 1) is largest over the canyon (U_3) with decreasing transport upstream (U_2) and downstream (U_4) of the canyon. A further transport decrease occurs at the upstream (U_1) and downstream (U_5) ends of the domain. Note that the downstream transports (U_4 and U_5) are slightly larger than the corresponding upstream values (U_1 and U_2), indicating some water movement onto the shelf from the ocean. The alongshore transport within the canyon (U_6 and U_7) are 4 to 5 times smaller than the flow along the shelf, but both are in the same direction as the alongshelf flow, becoming weaker with depth.

The transport across the shelf break at day 10 is an order of magnitude smaller than the alongshelf transports, with upstream values negative (onto the shelf) and downstream values positive. The largest cross-shore transports occur over the canyon above the shelf (V_2 and V_3), but significant transport crosses the shelf break upstream and downstream of the canyon (V_1 and V_4). Finally, there is small but nonnegligible transport within the canyon itself (V_5, V_7 and V_6, V_8).

These calculations indicate that the water is swirling around the canyon cyclonically; the magnitude of exchange in each direction across the shelf break is about the same. The small differences in the alongshore transport indicate that there is some net onshore water motion, but the magnitude is very small (less than 1% of the alongshore transport).

The vertical transport at day 10 is similar to the across-shelf transport, with downward motion on the upstream side (W_1 and W_3) and upward motion on the downstream side (W_2 and W_4). These values are about half of the across-shelf transport which indicates a substantial amount of water moving vertically within the canyon. However, the net vertical motion is small, given the slightly larger downward transport than the corresponding upward transport (W_1 versus W_2 and W_3 versus W_4). The initial downward adjustment of the isopycnals occurs during the first 5 days (both of the deep transports are downward), but thereafter, the circulation has no net vertical transport (Figure 7). Therefore the density field is displaced in the simulation only during the early spin-up and does not change thereafter.

3.5.2. Strongly stratified, downwelling. The transports at day 10 for the strongly stratified case are similar to those of the weakly stratified case, with only

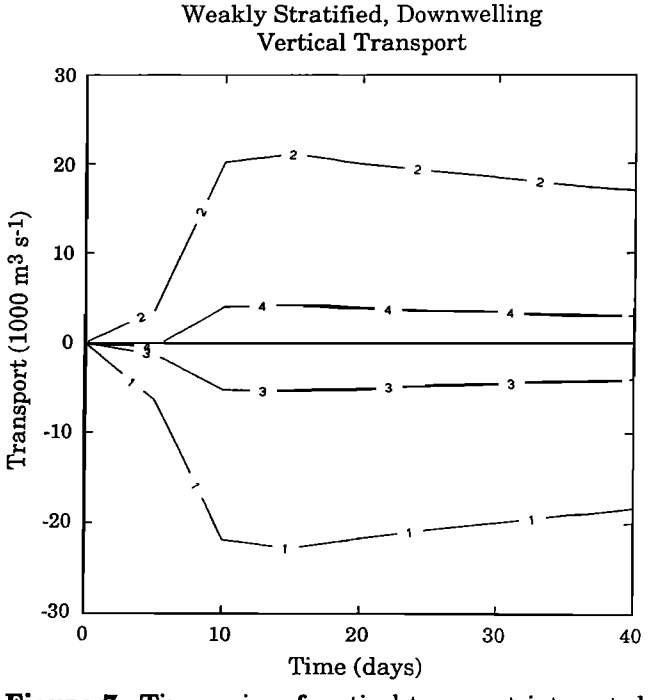

Figure 7. Time series of vertical transport integrated over the planes indicated in Figure 6 for the weakly stratified, downwelling case. The numbers on each line indicate which transport is being displayed. Values are plotted every 5 days.

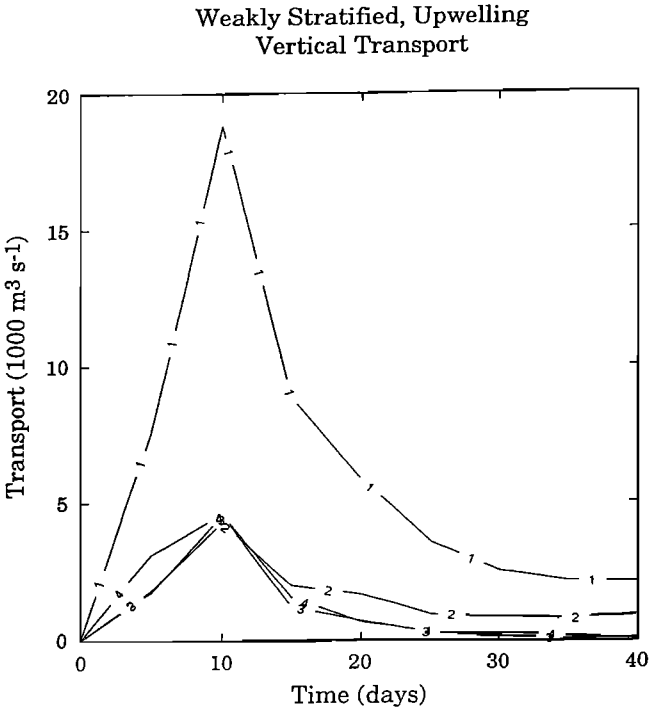

Figure 8. Same as Figure 7, except for the weakly stratified, upwelling case.

a few details being different (Table 1). The alongshore transport again is largest over the canyon (U_3) and weaker on either side, but the values at the five sections are much closer. Furthermore, the corresponding upsteam and downstream sections (U_2 versus U_4 and U_1 versus U_5) are essentially identical.

The transport across the shelf break is an order of magnitude smaller than the alongshelf values; upstream transport is onshore, while downstream is offshore. The largest transports are over the canyon above the shelf depth (V_2 and V_3) but the cross-shelf transports upstream and downstream of the canyon (V_1 and V_4) are significant. The transport within the canyon itself (V_5, V_7 and V_6, V_8) is a respectable fraction of that above the shelf break. The vertical transports are completely dominated by vertical motion at the shelf depth (W_1 and W_2), which are about the same magnitude and are comparable in size to the across shelf transport. The deeper vertical transports (W_2 and W_4) are negligibly small.

Two notable differences are caused by the higher stratification. A larger area is affected by the flow disturbance near the canyon, and the vertical motion in the canyon is more strongly confined to the upper water levels (above 150 m).

3.5.3. Weakly stratified, upwelling. The time behavior and magnitude of the transports for the weakly stratified, upwelling case are rather different from the downwelling cases just described. The vertical transports peak rapidly (Figure 8) and then decline to small values. The continual upwelling, however, distorts the isopycnals, creating baroclinic adjustment throughout the simulation. At day 10 the alongshore transport (Table 1) is everywhere negative, as expected, except for the deepest transport across the axis of the canyon (U_7), which is slightly positive, indicating a countercirculation deep in the canyon. The largest alongshore transport is now downstream of the canyon (U_1 and U_2), and the alongshore transport increases from upstream to downstream. There is very little difference in values between the ends of the domain and the edge of the canyon on the same side (U_1 versus U_2 and U_4 versus U_5), so the transport increase occurs by across-shelf flux at the canyon.

The across-shelf transports at day 10 are generally about a quarter of the alongshore values. Significant across-shore flow occurs over the canyon (V_2 and V_3). A weak onshore flow exists in the middle (V_5 and V_6) and deepest (V_7 and V_8) levels of the canyon. Over time, V_8 changes sign, indicating the development of a deep, baroclinic cyclone. The transports across the shelf break away from the canyon (V_1 and V_4) are small. The major cross-shelf exchange occurs above the shelf over the canyon.

The vertical transport tells a simple story (Figure 8), with upwelling everywhere and at magnitudes that are comparable to the largest onshore transports. The upward transport on the downstream side of the canyon (W_1) is largest by far, and the rest are about 5 times smaller. After the rapid increase during the first 10 days all of the vertical transports become smaller, eventually settling to a constant value toward the end of the simulation. There is persistent upwelling at the top of the canyon occuring at day 40, both on the up- and downstream sides of the canyon. The upwelling deeper in the canyon reduces nearly to zero.

3.5.4. Strongly stratified, upwelling. The case for strongly stratified upwelling is run for only 15 days, but the time behavior of the solution is similar to the weakly stratified case, only with smaller magnitudes. All of the alongshore transports at day 10 (Table 1) increase in the downstream direction, but the values away from the canyon on either side (U_1 and U_2, U_4 and U_5) are almost identical, indicating that there is very little water moving across the shelf break away from the canyon. The transport across the axis of the canyon below the shelf (U_6 and U_7) is very small, so the circulation within the canyon is very weak. The bulk of the onshore flow is occurring in the canyon, both above the level of the shelf (V_2 and V_3) and in the top 50 m of the canyon (V_5 and V_6). Small onshore flow also develops deep on the downstream side of the canyon (V_7), which is eventually balanced by outflow on the upstream side (V_8).

The vertical transports at day 10 indicate upwelling everywhere in the canyon, with the largest upwelling at the top of the downstream side of the canyon (W_1), but there is substantial upwelling on the upstream top of the canyon as well (W_2). The deeper vertical transports (W_3 and W_4) also indicate upwelling but much weaker than those higher up in the canyon.

4. Discussion

The first result of these simulations is the very different circulation that occurs with different direction of alongshore flow rather than with different stratification. It was originally thought that the important characteristic for canyons was the ratio of the canyon width to the internal radius of deformation and that a narrow canyon would respond very differently from a wide canyon. One way to characterize the stratification is through the stratification number ($S = NH/fL$), which is the ratio of the internal radius of deformation to a horizontal length scale, which in this case is the width of the canyon. For the simulations considered here the strongly stratified case does represent a narrow canyon (the canyon width is one third of the internal radius of deformation or $S = 3.3$), while the weakly stratified case is intermediate between wide and narrow (canyon width is about equal to the radius of deformation or $S = 0.82$).

Although the stratification does have some effect on the resulting circulation (see comments below), the direction of the alongshore flow is critical. For right-bounded coastal flow the geostrophic pressure gradient is offshore. As the flow at the shelf break turns toward the coast, it is slowed by the large-scale, cross-shore pressure gradient. This weakening of the flow reduces the Coriolis acceleration, allowing the water to be pushed offshore and down the topographic slope. After the water crosses the axis of the canyon, it is accelerated by the large-scale pressure gradient, rising due to the increased Coriolis acceleration. Because of the weak dissipation in these simulations, the water returns almost to its original depth (isobath), after which it continues alongshore. This circulation was observed by *Durrieu de Madron* [1994].

The large-scale, cross-shore pressure gradient is onshore for left-bounded flow and the same general dynamics described above apply. As the water enters the canyon from the shelf slope, it is now accelerated by the large-scale pressure gradient, sliding up the topography due to the increased Coriolis acceleration. Water near the top of the canyon is pushed onto the flat shelf and is no longer constrained to follow the canyon isobaths. The lifting of water on the upstream side of the canyon produces a large transport of water onto the shelf and is responsible for the fundamental difference in the circulation for the different directions of alongshore flow. Water deeper in the canyon is not lifted sufficiently to exit the canyon, and so it participates in the second phase of the circulation, where it is decelerated by the large-scale pressure gradient and pushed lower by the reduced Coriolis acceleration. The upwelling within the canyon is like that described by *Freeland and Denman* [1982], except that the water pooled near the head of the canyon in their case and the dense water was driven along the coast in these simulations.

For a given direction of alongshore flow, stratification controls the magnitude of the response, as is evident in the transport calculations. For the downwelling cases, increased stratification reduces the vertical transport by a factor of almost 3 and the cross-shore transport by half. The higher stratification also reduces the depth range over which the fluid parcels move in the circuit around the canyon. The upwelling cases have a similar reduction of the transport for increased stratification.

A second effect of stratification is to limit the influence of the canyon on the overlying flow. For downwelling cases the flow at middepth over the canyon is only weakly affected by the canyon, which is similar to the observations reported by *Hunkins* [1988] and *Noble and Butman* [1989], both of whom studied downwelling situations. As the stratification increases, the effect of the canyon decreases. For upwelling cases there is a similar decrease in the influence of the canyon on the overlying flow which agrees with observations [*Hickey et al.*, 1986; Hickey, submitted manuscript, 1995].

The structure of the flow in the canyon can be described by relative vorticity and vortex stretching. The downwelling cases have the simplest response. The fluid throughout the canyon is pushed deeper during its circuit, so there is a general downwelling in the canyon which stretches vortex columns near the surface. This stretching produces cyclonic vorticity which is evident in the circulation (Figure 2a). Further evidence of this circulation is given by the alongshore transport within the canyon (Table 1). The best indicators are U_6 and U_7, which are the transport in the top 50 m of the canyon and in the deep part of the canyon, respectively. For weakly stratified downwelling both of these values are consistent with cyclonic circulation throughout the canyon and a decrease in strength in the deeper part of the canyon. For the strongly stratified downwelling case the circulation is still cyclonic, with the upper circulation only half of that for the weakly stratified case. However, the deep circulation is considerably weaker with the increased stratification. *Hunkins* [1988] reports deep mean flow in the canyon to be weaker than that above, but there is no change in direction at the deepest level.

The upwelling case is more complicated because of the long-term baroclinic adjustment due to the continuing upwelling and the fact that the upstream flow is affected by the coastal plume. However, the circulation (Figure 4a) indicates an anticyclone on the shelf downstream of the canyon which is explained by compression of vortex columns by continuous upwelling at the top of the canyon. Since most of the lifting occurs at the head of the canyon, the vorticity is expressed on the adjacent shelf. At depths for which the water remains in the canyon, all of the vortex columns are stretched, giving rise to cyclonic vorticity (Figure 4b). *Freeland and Denman* [1982] report a cyclonic circulation over the canyon which is not consistent with the model results. It may be that the continuous upwelling in the model, coupled with export of the water along the coast, creates a different situation from the one observed by Freeland and Denman. The reason for this difference between model and observations is, at this point, not clear.

There is a second difference between the upwelling and downwelling cases; the upwelling cases have a reversal of the circulation deep in the canyon, while the downwelling cases do not. This result is unexpected but can be explained by considering two adjacent density layers. If the interface between the layers moves upward, then there is compression in the upper layer and stretching below, creating a change in sign of the vorticity in the two layers. This baroclinic response occurs in the upwelling cases. If, however, the upper surface moves downward a larger distance than the interface does, then there is compression in both layers and there is no reversal of the circulation. This barotropic response occurs in the downwelling cases. This difference in response between the two directions of coastal flow is due to the continual upwelling onto the shelf which creates large displacements of the isopycnals in the upper water column. In the downwelling cases the downward motion simply pools surface water over the canyon during the initial transient and the isopycnals thereafter cease moving which stops the vortex compression.

A result of this equilibrium in the downwelling cases as compared to upwelling is that there is a large difference in the amount of water moved across the shelf break for these two directions of coastal flow. In both of the downwelling cases the transport across the plane at the shelf break away from the canyon is weak. Over the canyon the transports are larger but are in both directions and therefore create very weak net exchange. The upwelling cases are very different in that some of the water that enters the canyon is deposited onto the continental shelf, creating a very large exchange, much larger than occurs across the shelf break away from the canyon.

Given that the flow speed in these simulations is of the order of 0.1 m s^{-1}, one might wonder about the importance of nonlinear processes. The Rossby number ($R_o = U/f\,L$) is an indicator of the importance of advection of momentum and has values ranging from 0.1 to 0.2, if the horizontal length scale is chosen to be the width of the canyon. Thus nonlinear effects are weak but not really negligible. The effect of advection of density is clearly important, especially in the upwelling case, where dense water is deposited onto the shelf by the circulation within the canyon.

An additional simulation was run for each of the upwelling cases in which momentum advection was removed from the model dynamics. The vertical speed at the top of the canyon (Figure 9), compared with the nonlinear case (Figure 5), covers a smaller area confined to the head of the canyon but is more intense. The flow is more symmetrical than the nonlinear case. Furthermore, the plume develops slower and propagates slower along the wall in the simulations without advection of momentum. The nonlinear processes do cause changes in the details of the circulation over the canyon. However, the solutions are not very different, indicating that the interaction of coastal flow, at least for the choices made in this study, are not strongly influenced by advection of momentum (the patterns are merely pushed downstream a bit) but are due to pressure gradients and Coriolis acceleration.

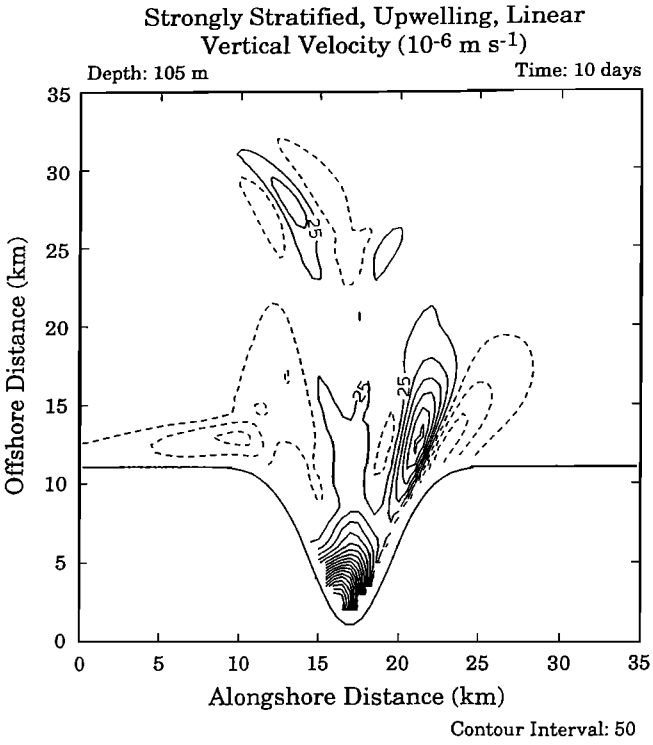

Figure 9. Same as Figure 3, except for the strongly stratified, upwelling case without momentum advection.

A number of physical processes were excluded from this dynamical study in order to sort out a small number of interactions. The most important process not included is vertical friction, which gives rise to frictional Ekman layers. The bottom frictional layer not only slows the flow, but also creates ageostrophic transports. The relative size of fluid transport across the shelf break away from the canyon by the bottom Ekman layer as compared with the transport within the canyon is important but cannot be estimated from this study. It would also be interesting to see if frictional slowing of the flow near the bottom causes fundamental differences in the circulation patterns. There are reports [*Hickey et al.*, 1986; *Durrieu du Madron*, 1994; Hickey, submitted manuscript, 1995] of detached nepheloid layers within canyons which are thought to come from frictional layers on the upstream corner of the canyon. Such processes are important to investigate but cannot be done with the current choice of dynamics.

These simulations have been forced in a very simple and, perhaps, unrealistic way by imposing a condition of total transport which gives rise to a very uniform and steady alongshore current. A better way to force the model would be with wind stress, which will create a more realistic structure to the alongshore flow. Winds also generate surface Ekman layers which provide another mechanism to transport water across the shelf break. Clearly, the next investigation should include vertical friction to allow both external forcing and

Ekman layers, which are both known to be important in coastal environments.

Another unrealistic feature of these simulations is that the alongshore flow is constant in strength throughout the simulation. Observations clearly show that the strength of the alongshore flow varies both with season and on timescales of days or weeks [*Hickey*, 1995, submitted manuscript, 1995]. This time variability means that it is unlikely that alongshore flow will persist for the long time used in the simulations. However, this time variability of the forcing can be considered only after steady circulation patterns have been analyzed.

Transport of water across the shelf break can also occur by flow variability due to instability of the shelf break front or instability of a strong offshore current. No instability occured in the alongshore flow in these simulations, so no statement can be made about the importance of these processes relative to the topographic interaction with the canyon. Flow instability is very difficult to investigate within numerical models because of the delicate nature of the dynamics that creates dynamic instability. The relative importance of canyon effects and instability at the shelf break cannot be investigated with the simulations included in this paper.

5. Conclusions

Before this modeling study it was thought that the parameter controlling the interaction of coastal flow with canyons was the stratification, specifically, the ratio of the internal radius of deformation to the canyon width. A wide canyon was thought to have a benign effect, merely steering the flow around the bathymetry, while a narrow canyon would create substantial exchange between the shelf and the ocean. The results of this study show that the canyon effect is controlled largely by the direction of the alongshore flow. In particular, right-bounded flow leads to shallow downwelling and weak exchange, while left-bounded flow creates upwelling and strong exchange across the shelf break.

The presence of stratification isolates the coastal flow from the influence of the canyon for the downwelling cases. In upwelling cases, dense water is pumped onto the shelf, even for strong stratification. However, the strength of the stratification determines the vertical distance over which the canyon affects the alongshore flow, with stronger stratification reducing the distance. For any stratification the surface temperature (density) is not modified at all by the flow interaction with the submarine canyon.

The important forces in these simulations are pressure gradients and Coriolis accelerations and how they interact with the bathymetric gradients. Advection of density is clearly important in the upwelling cases as a mechanism to change the density distribution. However, a simulation without advection of momentum indicates that this process is quite weak.

Finally, there is indication in these simulations that the transport of dense water onto the shelf in the upwelling cases removes energy from the alongshore flow and has the effect of retarding the coastal circulation. The true importance of this drag mechanism on coastal circulation must wait for simulations with direct forcing and viscous dissipation.

Acknowledgments. Most of the calculations in this paper were performed on the computers at the National Center for Atmospheric Research in Boulder, Colorado, which is supported by the National Science Foundation and at the Arctic Region Supercomputing Center in Fairbanks, Alaska. Additional computer facilities and support were provided by the Commonwealth Center for Coastal Physical Oceanography. This support is appreciated.

References

Durrieu de Madron, X., Hydrography and nepheloid structure in the Grand-Rhône canyon, *Cont. Shelf. Res.*, *14*, 457-477, 1994.

Freeland, H. J., and K. L. Denman, A topographically controlled upwelling center off southern Vancouver Island, *J. Mar. Res.*, *40*, 1069-1093, 1982.

Freeland, H., and P. McIntosh, The vorticity balance on the southern British Columbia continental shelf, *Atmos.-Ocean*, *27*, 643-657, 1989.

Haidvogel, D. B., J. L. Wilkin, and R. Young, A semi-spectral primitive equation circulation model using vertical sigma and orthogonal curvilinear horizontal coordinates, *J. Comput. Phys.*, *94*, 151-185, 1991.

Hickey, B., Coastal Submarine Canyons, *'Aha Huliko'a Winter Workshop on Flow Topography Interactions*, edited by P. Müller, pp. 1-16, Univ. of Hawaii, Honolulu, 1995.

Hickey, B., E. Baker, and N. Kachel, Suspended particle movement in and around Quinault Submarine Canyon, *Mar. Geol.*, *71*, 35-83, 1986.

Hunkins, K., Mean and tidal currents in Baltimore Canyon, *J. Geophys. Res.*, *93*, 6917-6929, 1988.

Inman, D. L., C. E. Nordstrom, and R. E. Flick, Currents in submarine canyons: An air-sea-land interaction, *Annu. Rev. Fluid Mech.*, *8*, 275-310, 1976.

Klinck, J. M., The influence of a narrow transverse canyon on initially geostrophic flow, *J. Geophys. Res.*, *93*, 509-515, 1988.

Klinck, J. M., Geostrophic adjustment over submarine canyons, *J. Geophys. Res.*, *94*, 6133-6144, 1989.

Noble, M., and B. Butman, The structure of subtidal currents within and around Lydonia Canyon: Evidence for enhanced cross-shelf fluctuations over the mouth of the canyon, *J. Geophys. Res.*, *94*, 8091-8110, 1989.

Wilkin, J. L., A computer program for calculating frequencies and modal structure of free coastal-trapped waves, *Tech. Rep. WHOI 87-53*, 50 pp., Woods Hole Oceanogr. Inst., Woods Hole, Mass., 1987.

Wilkin, J. L., and D. C. Chapman, Scattering of coastal-trapped waves by irregularities in coastline and topography, *J. Phys. Oceanogr.*, *20*, 396-421, 1990.

J. M. Klinck, Department of Oceanography, Center for Coastal Physical Oceanography, Old Dominion University, Norfolk, VA 23529. (e-mail: klinck@ccpo.odu.edu)

(Received March 13, 1995; revised August 31, 1995; accepted September 7, 1995.)